

Using γ +jets production to calibrate the Standard Model $Z(\rightarrow \nu\bar{\nu})$ +jets background to new physics processes at the LHC

S. Ask, M. A. Parker, T. Sandoval, M. E. Shea and W. J. Stirling

Cavendish Laboratory, University of Cambridge, CB3 0HE, UK.

ABSTRACT: The irreducible background from $Z(\rightarrow \nu\nu)$ +jets, to beyond the Standard Model searches at the LHC, can be calibrated using γ +jets data. The method utilises the fact that at high vector boson p_T ($\gg M_Z$), the event kinematics are the same for the two processes and the cross sections differ mainly due to the boson–quark couplings. The method relies on a precise prediction from theory of the Z/γ cross section ratio at high p_T , which should be insensitive to effects from full event simulation. We study the Z/γ ratio for final states involving 1, 2 and 3 hadronic jets, using both the leading–order parton shower Monte Carlo program PYTHIA8 and a leading–order matrix element program GAMBOS. This enables us both to understand the underlying parton dynamics in both processes, and to quantify the theoretical systematic uncertainties in the ratio predictions. Using a typical set of experimental cuts, we estimate the net theoretical uncertainty in the ratio to be of order $\pm 7\%$, when obtained from a Monte-Carlo program using multiparton matrix–elements for the hard process. Uncertainties associated with full event simulation are found to be small. The results indicate that an overall accuracy of the method, excluding statistical errors, of order 10% should be possible.

ARXIV EPRINT: [1107.2803](https://arxiv.org/abs/1107.2803)

Contents

1	Introduction	1
2	V+jets production in leading-order perturbative QCD	2
3	Parton level analysis	5
3.1	V + 1 jet results	6
3.2	Theoretical uncertainties	7
3.3	V + 2, 3 jets results	9
4	Full event simulation	13
4.1	Effects on the ratio	13
4.2	Background estimate for a zero lepton SUSY search	15
5	Summary and conclusions	19

1 Introduction

At the CERN Large Hadron Collider (LHC), $Z(\rightarrow \nu\bar{\nu})$ +jets is an important Standard Model (SM) background to new physics processes that give rise to missing transverse energy + jets signals. In principle, the related process $Z(\rightarrow e^+e^-, \mu^+\mu^-)$ +jets provides a way to calibrate this background, although in practice the number of such events may be too small to do this with sufficient precision. It has therefore been proposed [1–5] to use a related calibration process, γ +jets production, which has a much higher rate.¹ The key point is that at high transverse momentum, $p_T \gg M_Z$, γ and Z production are very similar; indeed the only expected difference in rate comes from the different electroweak couplings of photons and Z bosons to quarks, which are of course very well determined. There is also no branching ratio suppression for photon production. The *measured* rate of γ +jets production, coupled with theoretical knowledge of the *ratio* of Z and γ SM cross sections, can therefore be used to accurately predict the $Z(\rightarrow \nu\bar{\nu})$ +jets background.

Although the Z and γ cross sections have a simple theoretical relationship at high vector boson p_T , care is needed when estimating the theoretical ratio of Z and γ SM cross sections. Especially for more than one jet, there are matrix element contributions to the cross section that may not be included in parton shower Monte Carlos such as PYTHIA [7, 8] or HERWIG [9]. In addition, it is important to quantify the theoretical *uncertainty* on the ratio (from the choice of PDFs, QCD scales etc.), since this will propagate through to the overall uncertainty on the background estimate. A detailed theoretical study of the

¹The same technique has also been used by the CDF collaboration [6] to estimate a similar background in weak boson pair production in a hadronic final state at the Tevatron.

V + jets ($V = \gamma, Z$) cross sections and uncertainties is therefore required, to supplement the information from Monte Carlo event simulation. Finally, it is important to establish how well the theoretical precision survives under conditions closer to the experimental analysis, e.g. including effects from full event simulation, jet reconstruction, detector acceptance, experimental cuts etc.

In this paper we report on such a study. Since our main interest is in estimating the missing E_T distribution in events with multijets, we focus primarily on the inclusive vector-boson (Z or γ) transverse momentum (p_T) distributions, particularly at high $p_T \gg M_Z$. We first analyse the ratio of the $Z+1$ jet and $\gamma+1$ jet p_T distributions from a general theoretical perspective using a program for up to and including 3 jets based on exact leading-order parton-level matrix elements. We then reproduce these results using PYTHIA8 [7, 8] (at parton level). This establishes that the ratio of the two process cross sections is theoretically robust, particularly at high p_T . We predict the value of the cross section ratio using ‘typical’ experimental cuts, and estimate its theoretical uncertainty. We then consider the corresponding 2- and 3-jet cross sections, again comparing the exact leading-order matrix element results with those obtained from PYTHIA8. Finally, we use our results to assess the systematic uncertainties on the missing transverse energy + jets background obtained from the photon + jets cross section using this method. The ratios predicted by the two alternative approaches, based on “pure” matrix elements or parton showers, are illustrated as well as used to constrain the systematic uncertainties related to the commonly used, and also more optimal, scenario where matrix elements are matched with the parton shower used in the MC simulation. In the following sections, V refers to the vector bosons Z or γ .

In a recent paper [10], a similar study was carried out for the $V + 2$ jets cross sections using two approaches: next-to-leading order in pQCD applied at parton level, and exact leading-order matrix elements interfaced with parton showers (ME+PS) as implemented in SHERPA [11]. Agreement between our results and those of [10] confirms that over much of the relevant phase space, and particularly for inclusive quantities, the effect of higher-order corrections on the leading-order Z, γ cross section ratios is small. In our study, we consider also the 1- and 3-jet ratios and, more importantly, we extend the analysis to hadron level using PYTHIA8. This allows for an analysis similar to the ones within the LHC experiments. We also examine the dependence of the ratios on the parton distribution functions, since these receive different weightings in the Z and γ cross sections and therefore do not exactly cancel in the ratio. Of course ultimately one would wish to evaluate all these cross sections consistently at next-to-leading order, using the methods described in [10] for the 2-jet case.

2 V +jets production in leading-order perturbative QCD

In the Standard Model, the coupling of photons and Z bosons to quarks q are, respectively,

$$-ieQ_q\gamma^\mu \quad \text{and} \quad \frac{-ie}{2\sin\theta_W\cos\theta_W}\gamma^\mu(v_q - a_q\gamma_5), \quad (2.1)$$

where Q_q , v_q and a_q , are respectively the electric, vector and axial neutral weak couplings of the quarks, and θ_W is the weak mixing angle. For hadron collider processes such as

$q\bar{q} \rightarrow V + ng$ or $qg \rightarrow qV + (n-1)g$, both of which contribute to $V + n$ jets production, the matrix elements squared will contain factors of Q_q^2 or $(v_q^2 + a_q^2)/4 \sin^2 \theta_W \cos^2 \theta_W$ for γ or Z respectively. The only other difference in the matrix elements comes from the non-zero Z mass², which will appear in the internal propagators and phase space integration. Sample Feynman diagrams for $V + 1$ jet production are shown in figures 1(a,b), and for $V + 2$ jet production in figures 1(c-f).

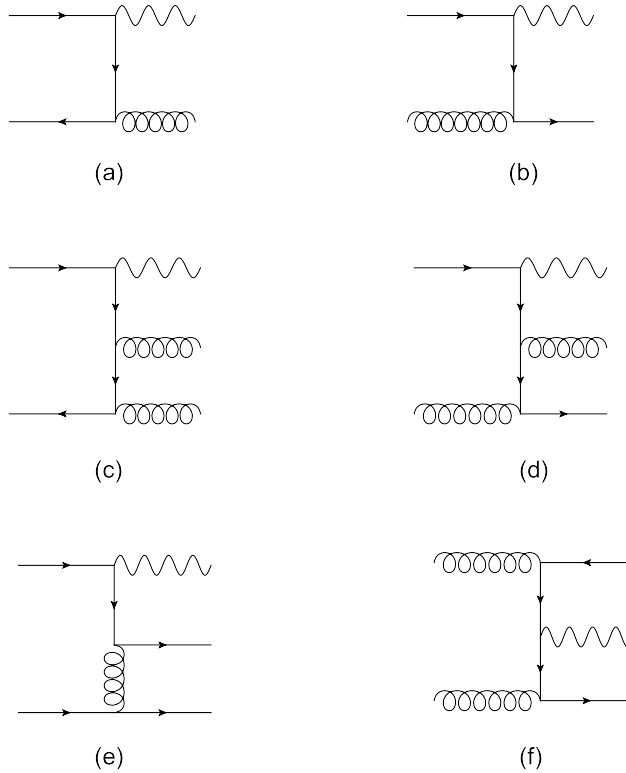


Figure 1. Sample Feynman diagrams for $V + 1, 2$ jets production, where $V = \gamma, Z$.

For high $p_T(V)$ ($\gg M_Z$) production we would therefore expect the Z and γ cross sections to be in the ratio

$$R_q = \frac{v_q^2 + a_q^2}{4 \sin^2 \theta_W \cos^2 \theta_W Q_q^2}. \quad (2.2)$$

Substituting $\sin^2 \theta_W = 0.2315$, we obtain $R_u = 0.906$ and $R_d = 4.673$. In practice, of course, the cross sections will receive contributions from *all* quark flavour types, and so $R = \sigma(Z)/\sigma(\gamma)$ will be a weighted average of the R_u and R_d values, i.e.

$$R = \frac{Z_u \langle u \rangle + Z_d \langle d \rangle}{\gamma_u \langle u \rangle + \gamma_d \langle d \rangle} \quad (2.3)$$

²For the purposes of this discussion, we treat the Z as an on-shell stable particle. In practice, Z decay will also form part of the matrix elements.

in an obvious notation, where $\langle u \rangle$ and $\langle d \rangle$ are the typical values of the u -type and d -type quark parton distribution functions (PDFs) in the cross section. Figure 2(a) shows R as a function of the ratio $\langle d \rangle / \langle u \rangle$. We would expect that where large x values are probed, for example at very high $p_T(V)$, the ratio would approach the R_u value since $d(x)/u(x) \rightarrow 0$ as $x \rightarrow 1$, see figure 2(b). For moderate p_T values at the LHC, $\langle x \rangle \sim 0.1$, which corresponds to $\langle d \rangle / \langle u \rangle \simeq 0.6$ and therefore $R \simeq 1.4$.

The simple connection (2.3) between the vector boson cross section ratio and the initial state quark flavour is, however, broken for $n_{\text{jets}} \geq 2$. Consider for example the sample Feynman diagrams of figure 1(e) and (f). For the former ‘four-quark’ diagrams, the vector boson can be emitted off any of the external quark legs and so the numerator and denominator of the ratio R depend on more complicated products of quark distributions. Because at high x uu scattering will be relatively more dominant than dd scattering, we would expect that the value of R for such processes would be closer to R_u than to R_d , compared to the 1-jet ratio. On the other hand, for the gg -scattering diagrams, figure 1(f), the ratio of the corresponding cross sections is (ignoring the Z mass) $R = \sum_q Z_q / \sum_q \gamma_q$, where the sum is over the final state quark (antiquark) flavours, and the dependence on the initial state (gluon) distributions cancels. By way of illustration, with 5 massless flavours we obtain $R = 1.933$. As we shall see below, the four-quark contribution is more important at high p_T than the gg contribution, and the net effect is to reduce R slightly compared to the 1-jet case.

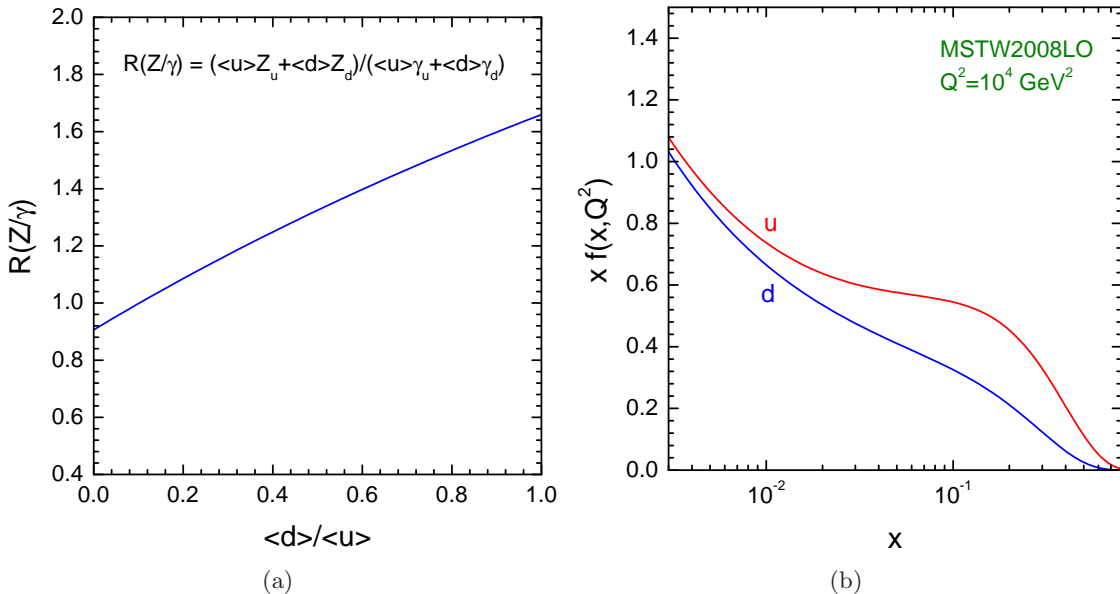


Figure 2. (a) Dependence of $R = \sigma(Z)/\sigma(\gamma)$ at the coupling constant level on the ratio of average d and u parton distribution values, see eq. 2.3. (b) u and d quark MSTW2008LO PDFs [13] at $Q^2 = 10^4 \text{ GeV}^2$.

Figure 3(a) shows the $Z + 1$ jet and $\gamma + 1$ jet cross sections³ as functions of the vector

³Expressions for the matrix elements can be found, for example in Chapter 9 of [12].

boson transverse momentum at $\sqrt{s} = 7$ TeV and 14 TeV. Standard PDG values of the electroweak parameters are used, and the PDFs are the leading-order MSTW2008LO set [13] with renormalisation and factorisation scale choice $\mu_R = \mu_F = p_T(V)$, and the Z is treated as an on-shell stable boson. The acceptance cuts are $|y(V, j)| < 2.5$ and $p_T(V, j) > 40$ GeV, where y is the rapidity. Figure 3(b) shows the ratio of the Z and γ distributions. We see the expected behaviour of a roughly constant ratio at large $p_T(V) \gg M_Z$ lying between the R_u and R_d values defined above. Although above $p_T \sim M_Z$ the ratio does exhibit a plateau region, at very large p_T we begin to see a slight decrease, as the high- x behaviour of the d/u PDF ratio drives the ratio down towards the R_u value. At 14 TeV, the empirical large- p_T value of $R \simeq 1.4$ is consistent with $\langle d \rangle / \langle u \rangle \simeq 0.6$, see figure 2(a). This in turn is consistent with u and d PDFs probed in the $x \sim 0.1$ region, see figure 2(b). At the lower collider energy (7 TeV), higher x values are sampled for the same p_T , and the Z/γ ratio decreases slightly, moving towards the R_u value. Note that the ratio curves in figure 3(b) can be reasonably well approximated by

$$R = R_0 \left(\frac{p_T^2}{p_T^2 + M_Z^2} \right)^n, \quad (2.4)$$

with $n \approx 1.2$, illustrating the expected Z mass suppression relative to the photon distribution for $p_T < M_Z$.

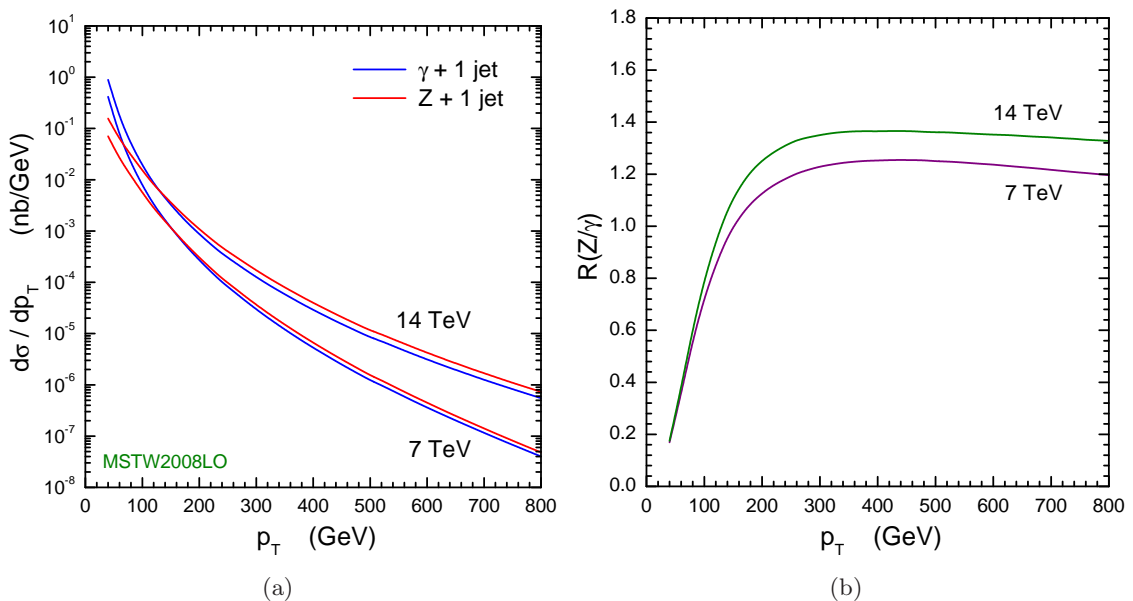


Figure 3. (a) Z and γ p_T distributions at $\sqrt{s} = 7$ TeV and 14 TeV, with parameters and cuts as described in the text. (b) Ratio of the Z and γ p_T distributions.

3 Parton level analysis

In order to study the ratio of the Z and γ distributions in a realistic experimental environment, we need to use an event simulation Monte Carlo program. We use PYTHIA8 for this

purpose. At the same time, we want to understand the difference between the scattering amplitudes embedded in PYTHIA8 and the amplitudes obtained using exact QCD matrix elements for multijet production. For the latter we use the program GAMBOS, an adaptation of the Giele et al. VECBOS program [14] for $W, Z + n$ jets production, in which the weak boson is replaced by a photon.

First, we compare the PYTHIA8 and GAMBOS results at the parton level. This serves to check the consistency of the results from the two programs, when configured as similarly as possible, and provides a common middle step between the matrix-element (ME) $V +$ jets results at parton level produced by GAMBOS and the results for fully simulated events from PYTHIA8.

The PYTHIA8 results are obtained using the LO ($2 \rightarrow 2$) processes, $q\bar{q} \rightarrow Vg$ and $qg \rightarrow Vq$ where $V = \gamma$ or Z , corresponding to the Feynman diagram types shown in figures 1(a,b). Events with ≥ 2 jets are generated by parton showering off the initial and final state partons. This means that processes such as those shown in figures 1(c) to 1(f) are included, albeit with an approximation to the exact matrix elements, and we can therefore expect differences between GAMBOS and PYTHIA8 results for the Z/γ ratios with ≥ 2 jets.

In order to produce results directly comparable with GAMBOS, the following settings are used as default in PYTHIA8:

- **PDFs:** MSTW2008LO;
- **Strong:** $\alpha_S(M_Z^2) = 0.13939$, with one loop running;
- **EM:** $\alpha_{EM}(M_Z^2) = 1/127.918$, with one loop running;
- **Weak:** $\sin^2(\theta_W) = 0.2315$;
- **Scales:** Renormalisation and factorisation scales, $\mu_R = \mu_F = p_T(V)$;
- **Rapidity, transverse momentum and separation cuts** on the final-state Z, γ and jets as described in the previous section.

In the following sub-sections we first compare results for the $V + 1$ jet distributions, then discuss the theoretical uncertainties on the corresponding Z/γ ratio, and finally compare the $V + 2, 3$ jet results from the two programs.

3.1 $V + 1$ jet results

The LO matrix elements used in the PYTHIA8 processes are the same as those used in GAMBOS for the $V + 1$ jet case, and a parton level comparison between the two programs should therefore give identical results. Note that the V and the jet correspond to the outgoing partons of the hard process in PYTHIA8, without any further simulation of the event. The differential Z and γ cross sections and their ratio predicted by PYTHIA8 are shown in figure 4 for pp collisions at 7 as well as 14 TeV. The results show the same characteristic features already seen in the GAMBOS predictions in figure 3, i.e. the Z cross section, excluding any branching ratios, is smaller than the photon cross section at small p_T due to the mass suppression, but is roughly proportional to, and slightly larger than,

the γ cross section at $p_T \gg M_Z$. The ratios obtained from PYTHIA8 and GAMBOS are compared in figure 5, for 7 TeV and 14 TeV collision energies. Evidently there is good agreement between the two programs, as expected. As seen in the plot, the photon cross sections from the two programs agree perfectly, whereas a small difference between the Z cross sections, $<5\%$, is visible. This difference is due to the way in which the PYTHIA8 generator treats the Z boson as a resonance, in contrast to GAMBOS where the Z is treated as a real particle, and this was confirmed by producing a GAMBOS like process in PYTHIA8 which reproduced the same results. Since the Z boson is generally treated as a resonance in MC programs, this difference is not considered as a source of uncertainty.

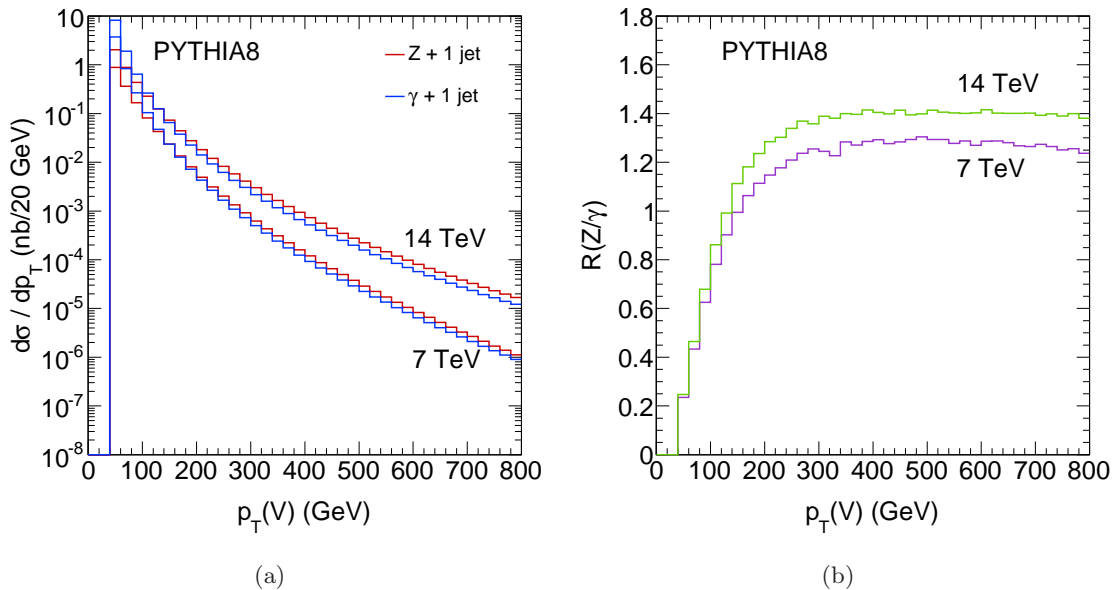


Figure 4. (a) Differential cross section as a function of the vector boson p_T for the process $pp \rightarrow V + 1$ parton with $V = \gamma, Z$ from PYTHIA8, and (b) the ratio of these.

3.2 Theoretical uncertainties

Having established numerical agreement between the two programs, we can use PYTHIA8 to investigate the theoretical uncertainty on the Z/γ ratio at high p_T . There are a number of sources of these, which we address in turn.

First, we consider the dependence on the PDFs used in the calculation. As argued in section 2, the Z/γ ratio at high p_T is sensitive to the d/u parton ratio at large x . To study the possible variation in this ratio, we investigate the spread from using the different eigenvectors of the MSTW2008LO set and we compare these predictions with those from two (older) leading-order PDF sets, CTEQ5L [15] and GRV98 [16], shown in figure 6. The latter should yield a *conservative* estimate of the PDF dependence. The impact on the Z and γ distributions and their ratio is shown in figure 7. Note that the CTEQ5L and GRV98 PDFs give respectively softer and harder Z and γ p_T distributions, which is an artefact of the underlying quark and gluon PDF behaviour, see figure 6(a), but that the

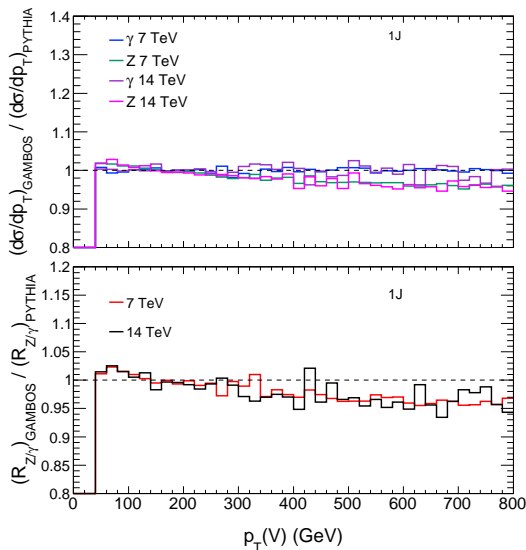


Figure 5. Effect on the boson p_T and the ratio from using a matrix–element generator (GAMBOS) and PYTHIA8 at 7 and 14 TeV.

effect largely cancels in the ratio. The residual small differences in the cross section ratio can be understood in terms of the corresponding small differences in the d/u ratio for the various sets, shown in figure 6(b). We ascribe a conservative $\pm 4\%$ PDF uncertainty to the $R(Z/\gamma)$ ratio at high $p_T(V)$.

In addition to varying the PDFs, we use different choices for the renormalisation and factorisation scales, μ_R and μ_F , in order to mimic the effect of higher–order pQCD corrections not included in either the PYTHIA8 or GAMBOS analyses. In particular, we use multiples of the default scales $\mu_R = \mu_F = p_T(V)$, and two variants of this: the arithmetic and geometric means of the final-state transverse masses in the $2 \rightarrow 2$ hard process, $\mu_{\text{ari}}^2 = (m_{T1}^2 + m_{T2}^2)/2 = (2p_T(V)^2 + m(V)^2)/2$ and $\mu_{\text{geo}}^2 = m_{T1}m_{T2} = p_T(V)\sqrt{p_T(V)^2 + m(V)^2}$. Note that for the photon, these scales are identical to the default scale $p_T(\gamma)$. Figure 8 presents the corresponding impact on the differential cross sections, $d\sigma/dp_T$, as well as the cross section ratio, $R(Z/\gamma)$. The results show that although the variations have significant effects on the differential cross sections, as expected, the Z/γ ratio remains stable in the regime $p_T \gg M_Z$, and for $p_T(V) > 100$ GeV all variations of the ratio are within $\pm 3\%$.

Indeed the only sizable effect on the ratio related to the scales is observed from the different choices of the scale μ_R , which becomes visible at $p_T \ll M_Z$. Any choice of scale of the form κp_T will of course cancel in the Z/γ ratio, but scales of the form $\kappa\sqrt{p_T^2 + M_V^2}$ will give different results for low $p_T \sim M_V$. The size of this effect was also shown to be consistent with the ratio $\alpha_S(\mu_R(Z))/\alpha_S(\mu_R(\gamma))$ using the same one–loop formula as in PYTHIA8 and GAMBOS. No similar effects are observed from different choices of the factorisation scale μ_F , since the PDFs vary only weakly with the factorisation scale at the x values probed by these cross sections.

Note that in the above analysis we have used the *same* form of scale variation simul-

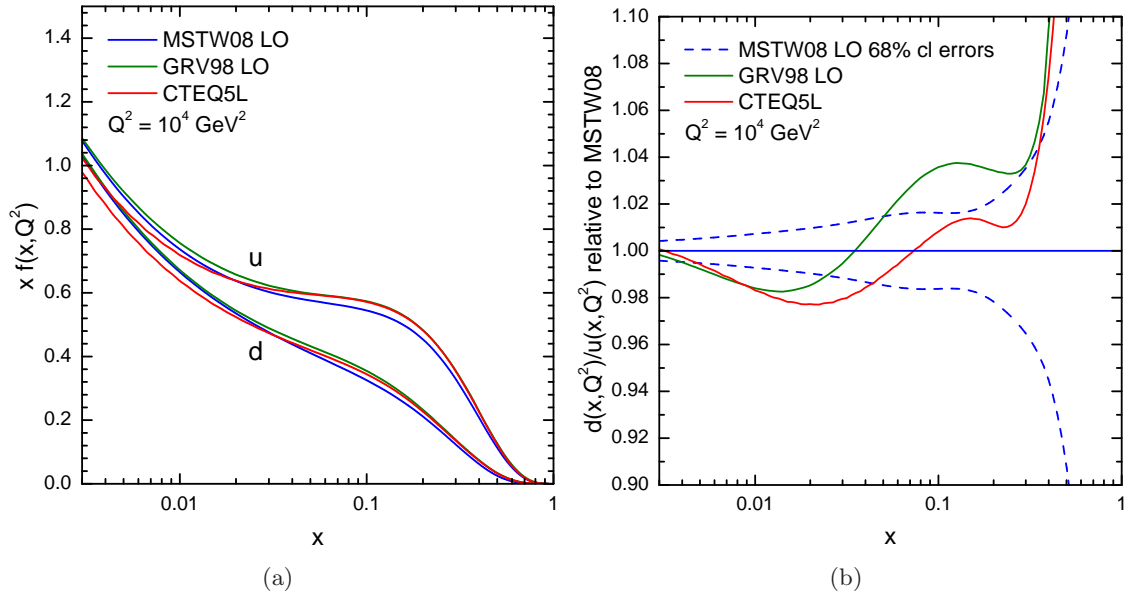


Figure 6. (a) Comparison of up and down quark distributions from MSTW2008LO, CTEQ5L and GRV98. (b) d/u ratios compared to MSTW2008LO.

taneously in both the numerator (Z) and denominator (γ) cross sections. As pointed out in Ref. [10], this gives a much smaller scale variation than if the scales are varied *independently* in the two cross sections. However, we argue that if we select Z and γ events for which the kinematics of the (colour-singlet) vector bosons and the jets are the same, and if the energies and momenta are large enough such that the Z mass can be neglected (e.g. $p_T \gg M_Z$), then the higher-order pQCD corrections to both cross sections should essentially be the same and should therefore largely cancel in the ratio.

3.3 $V + 2, 3$ jets results

For the $V + 2$ jets production cross sections there is an additional complication in that the high- p_T photon can be emitted collinearly to a high- p_T quark, with the transverse momentum of the pair being balanced by an ‘away side’ quark or gluon. For massless photons, quarks and gluons the matrix element is singular in this configuration and so the closer the photon is allowed to approach the quark, the smaller the Z/γ ratio becomes, since there is no such collinear singularity for Z production. To regulate the singularity, we impose a $\Delta R(V, j) > \Delta R_{\min}$ isolation cut, where $V = \gamma, Z$ and $j = q, g$.⁴ We also, of course, need to impose rapidity, transverse momentum and jet-jet separation cuts on the quark

⁴Note that the requirement of photon isolation becomes more subtle beyond leading order in pQCD, since in this case the partonic jets can have non-zero ‘width’ and the choice of jet algorithm influences the analysis. This issue is addressed in detail in Ref. [10]. In our case we will be studying photon isolation for the full PYTHIA8 event simulation including hadronisation and experimental cuts. Note also that we neglect contributions to the γ cross section involving photon fragmentation functions, i.e. $f^{q \rightarrow \gamma}(z, Q^2)$. With the strong isolation requirements and high transverse momentum values used in our study, we expect such contributions to be small.

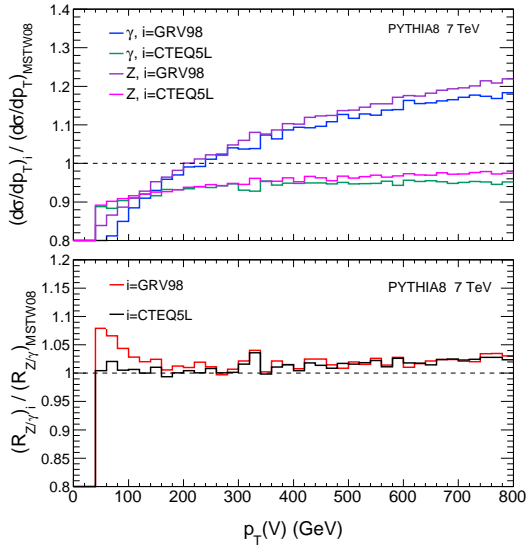


Figure 7. Effects on (Z, γ) differential cross sections and cross section ratio after varying the PDFs

and gluons jets. For illustration, we choose $p_T(j) > 40$ GeV, $|y(j)| < 2.5$ (as for the 1-jet study above), and $\Delta R(j, j) > 0.4$ to represent ‘typical’ experimental cuts. Figure 9(a) shows the ratio of $V + 2$ jet cross sections, as calculated using GAMBOS, for different values $\Delta R_{\min} = 0.05, 0.1, 0.2, 0.4, 0.6$ at 7 TeV. The ratio at high p_T shows the expected dependence on the minimum separation. Note also that the ratio becomes insensitive to the isolation cut when the minimum separation becomes large, since far from the singularity the Z and γ phase space are affected more or less equally. A similar dependence on ΔR_{\min} is observed for the $V + 3$ jet ratios. From now on we take $\Delta R_{\min} = 0.4$ as our default choice and attribute a $\pm 5\%$ uncertainty of these results based on the difference with respect to $\Delta R_{\min} = 0.6$.

The breakdown of the $Z + 2$ jet GAMBOS cross section at 7 TeV into the different subprocess contributions is shown in figure 9(b). We define these to be $q\bar{q} \rightarrow Vgg$ scattering (e.g. figure 1(c)), $qg, gq \rightarrow Vqq$ (e.g. figure 1(d)), $gg \rightarrow Vq\bar{q}$ (e.g. figure 1(f)) and $qq \rightarrow Vqq$ (e.g. figure 1(e)), where a sum over quarks and antiquarks is implied. Note that quark–gluon scattering is by far the most dominant in the kinematic region studied here, and its fractional contribution is roughly independent of $p_T(V)$. The results also show that the second largest contribution in the 2-jets case comes from the qq subprocess, which approximately amounts to 20%. This is in contrast to the 1-jet case, which is dominated by qg and $q\bar{q}$ scattering. The corresponding subprocess breakdown of the $\gamma + 2$ jet cross section is similar.

In figure 10(a) we show the $Z/\gamma + 1, 2, 3$ jet GAMBOS cross section ratios as a function of $p_T(V)$, with $\Delta R_{\min} = 0.4$ and other cuts as before. We see that the 2,3 jet ratios are slightly smaller than the 1 jet ratio at moderate and high p_T . The small difference arises from three effects: (i) the dependence of the 2,3 jet cross sections on $\Delta R_{\min} = 0.4$, (ii) the additional qq and gg scattering diagrams, the net effect of which is to decrease the 2,3 jet

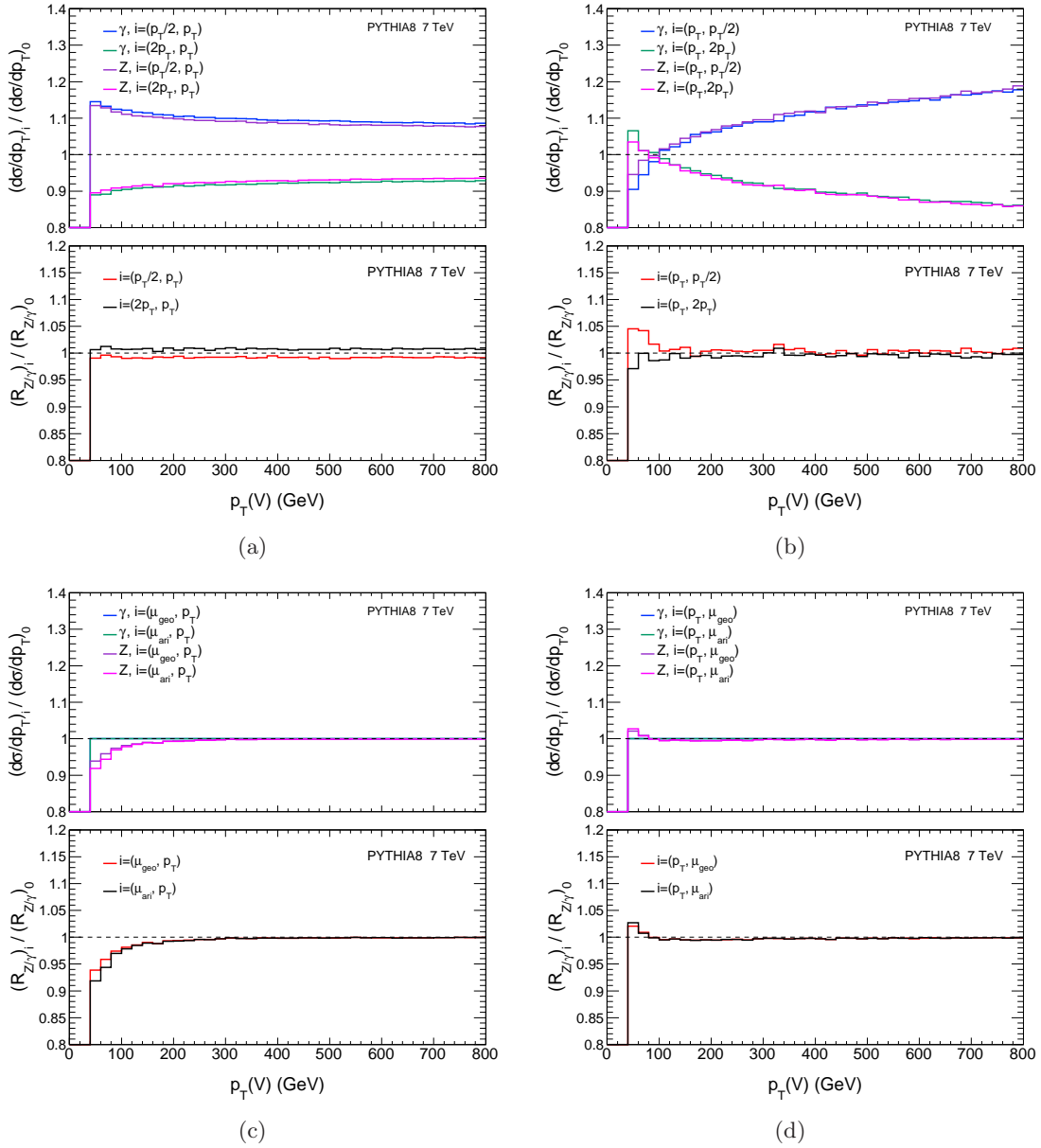


Figure 8. Effects on (Z, γ) differential cross sections and cross section ratio after varying the scales (μ_R, μ_F) . The different μ scales are defined in the text and the denominators correspond to using the default scale choice, i.e. $0 = (p_T, p_T)$.

ratio, as already explained in section 2, and (iii) the fact that for a fixed p_T , increasing the number of jets increases the overall invariant mass of the final-state system, and also therefore the values of the parton momentum fractions. This in turn decreases the d/u ratio, and also the Z/γ ratio, see figure 2(a).

For more than one jet, the additional jets in the PYTHIA8 simulation are produced by parton showering. In order to characterise the difference with respect to exact MEs, the

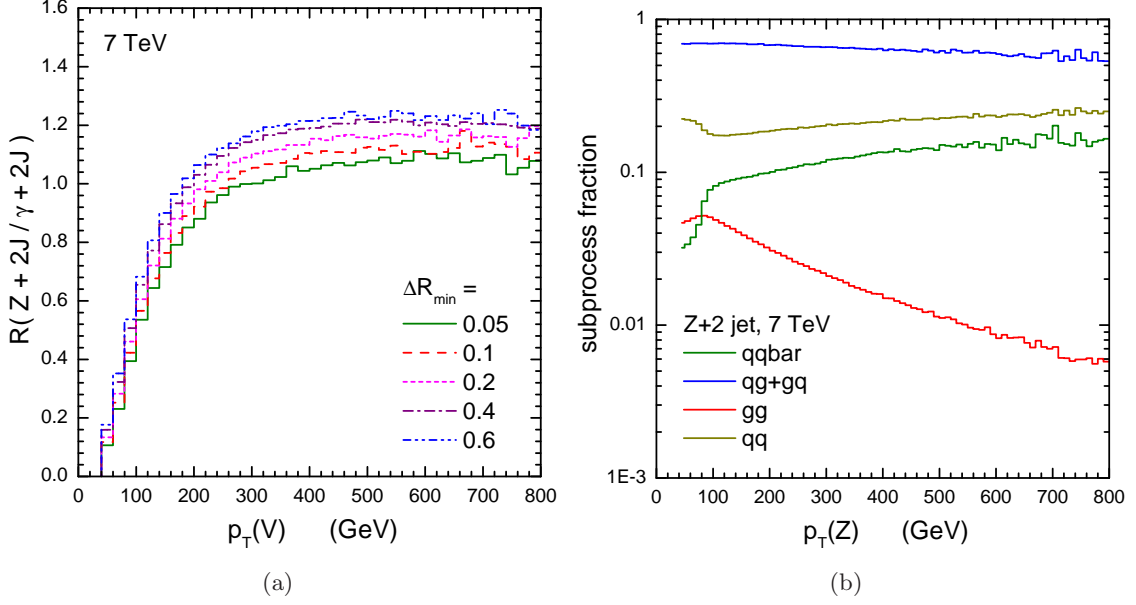


Figure 9. (a) Ratio of the $Z + 2$ jets and $\gamma + 2$ jets $p_T(V)$ distributions at 7 TeV, for different values of the $\Delta R(V, j) > \Delta R_{\min}$ isolation cut. (b) Breakdown of the $Z + 2$ jet GAMBOS cross section into the different subprocess contributions defined in the text.

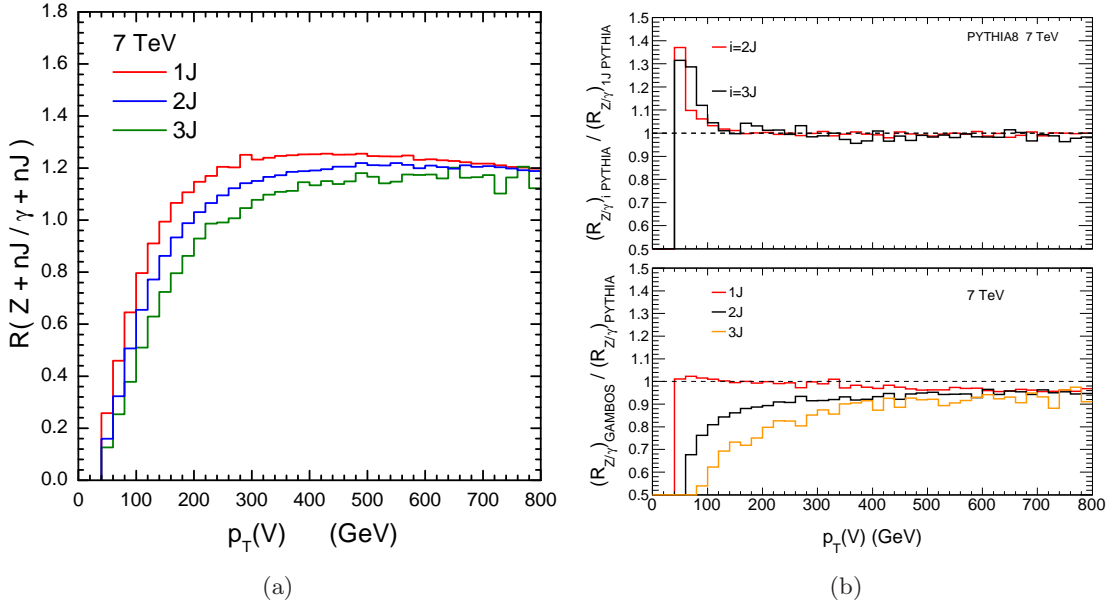


Figure 10. (a) $Z/\gamma + 1, 2, 3$ jet GAMBOS cross section ratios as a function of $p_T(V)$, with the isolation cut $\Delta R_{\min} = 0.4$. (b) Effect from multijet requirement on the PYTHIA8 ratio (upper) and difference with respect to GAMBOS (lower).

following events were used for the 2- and 3-jet results from PYTHIA8 at the parton level, where the aim is to produce events with a similar parton level topology to the GAMBOS

events based on the multijet MEs. In the 2-jet case, events were generated with both initial (ISR) and final state radiation (FSR) enabled and only those with exactly 2 jets within the allowed p_T and y acceptance were considered. These jets either correspond to the parton from the hard scatter together with an ISR emission or from events with no accepted ISR emission, but where the hard parton, due to FSR, branches into two partons within the allowed acceptance. In addition, only events with the required V -jet and jet-jet ΔR separation were considered. The same event selection was used for the parton level 3-jet case, where the three jets either correspond to the hard parton together with two ISR emissions, or a FSR branch of the hard parton together with one ISR emission, or two FSR emissions. The multijet ratios from PYTHIA8 were found to be very similar to the one jet case. This is illustrated in the upper plot of figure 10(b), which shows the PYTHIA8 $R_{2\text{jet}}/R_{1\text{jet}}$ and $R_{3\text{jet}}/R_{1\text{jet}}$ ratios.⁵ The corresponding GAMBOS Z/γ ratios are therefore slightly smaller as shown in the lower plot of figure 10(b). These results illustrate the difference between the two individual approaches in the multijet case as well as the importance of using a multiparton ME based program in the actual analysis, where the precision related to the ME calculation was discussed above in connection with figure 9. By comparing the GAMBOS and PYTHIA8 ratios at high p_T , we can extract correction factors for the PYTHIA8 ratios to take account of the missing contributions, however, as seen in figure 10(b) these correction factors are not large.

4 Full event simulation

The ability of PYTHIA8 to simulate full events was used both to investigate the robustness of the Z/γ cross section ratio as well as its potential use in estimating the $Z \rightarrow \nu\bar{\nu}$ background in searches for new physics at the LHC. For simplicity, the experimental aspects related to the photon analysis attempt to follow as closely as possible what is commonly used in ATLAS analyses [17, 18], and for the new physics scenario we focus on the SUSY zero-lepton search [1, 2], where SM $Z \rightarrow \nu\bar{\nu}$ production is one of the main backgrounds. Due to the phenomenological nature of this study, we neglect any experimental photon inefficiencies, apart from the isolation criteria discussed below, as well as any backgrounds (e.g. $\pi^0 \rightarrow 2\gamma$), which in any case are expected to be relatively small in the high p_T region of interest.

4.1 Effects on the ratio

The same PYTHIA8 processes were used as in the parton-level study, but with the full parton shower, hadronisation, multiple interaction and particle decay simulation enabled. The default settings of v8.150 were used, for which general performance results can be found in [19]. The same selection was used as for the 1-jet parton-level results, here corresponding

⁵The large deviation in the first bins is an artefact of the kinematic acceptance. In the 1-jet case, events will populate these bins according to the normal underlying distribution. However, since shower emissions can only occur with p_T smaller than the hard process, the 2,3 jet events will be peaked toward the upper bin edge. Due to the sharp rise of the ratio at low p_T , the average ratio value in these bins will therefore be significantly different for the higher jet multiplicities.

to an inclusive jet selection. The main differences with respect to the parton-level results come from using the final state boson momentum as well as from using jets reconstructed from the final state particles, rather than being represented by single partons. The jets were reconstructed using the FASTJET library [20–22] and were based on all final-state particles except leptons and any photons with $p_T^\gamma > 30$ GeV. The anti- k_t algorithm was used with a R parameter of 0.4, also in accordance with the ATLAS analysis. In the following, these results from full event simulation are referred to as obtained at particle level.

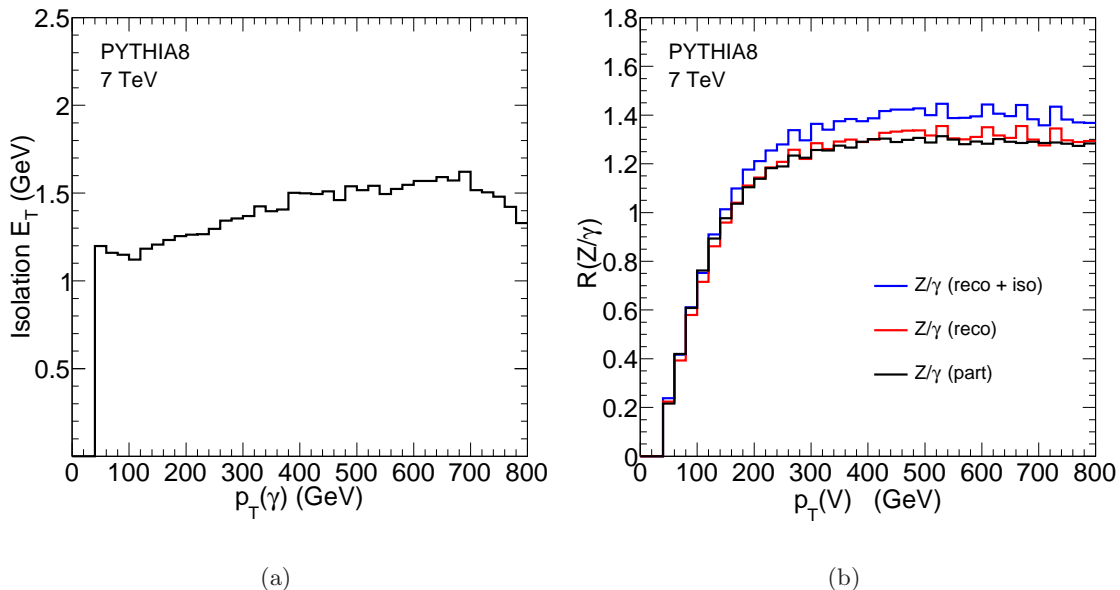


Figure 11. (a) Transverse energy inside the photon isolation cone as a function of the photon p_T . (b) Z/γ cross section ratio as a function of the photon p_T . Parton (part) and particle level results (reco) are shown as well as for events passing the isolation criteria (reco + iso).

The experimental analysis in ATLAS uses a photon isolation criterion in order to suppress QCD background and this quantity was found to be well described at MC generator level. This isolation criterion requires the transverse energy within a $\Delta R[= \sqrt{\Delta\eta^2 + \Delta\phi^2}] = 0.4$ cone around the photon (E_T^{iso}) not to exceed 4 GeV. Since the anticipated use of the ratio here is to estimate the number of Z events from measured γ events, the effect from this isolation requirement is also addressed. The fact that only isolated photons are considered implies an even stronger photon-jet separation than the one used above for the parton level results, ensuring an acceptance where GAMBOS provides robust calculations. The mean transverse energy within the photon isolation cone is shown in figure 11(a) as a function of the photon p_T . This plot is based on events which pass the above selection applied to the final state photon as well as the reconstructed jets. A small increase with p_T is shown, but with values well below 4 GeV over the whole range. In spite of the increasing hadronic recoil with larger boson p_T , a relatively constant inefficiency of about 5% was found over the full p_T range.

Figure 11(b) shows the Z/γ cross section ratio at parton (part) and particle level (reco)

as well as at particle level where the isolation requirement is applied (reco+iso). Good agreement is evident between the results obtained at parton and particle level, where the difference is well below 5% at high p_T , and the increase of the ratio due to the photon isolation criterion is of order 6% at high p_T .

4.2 Background estimate for a zero lepton SUSY search

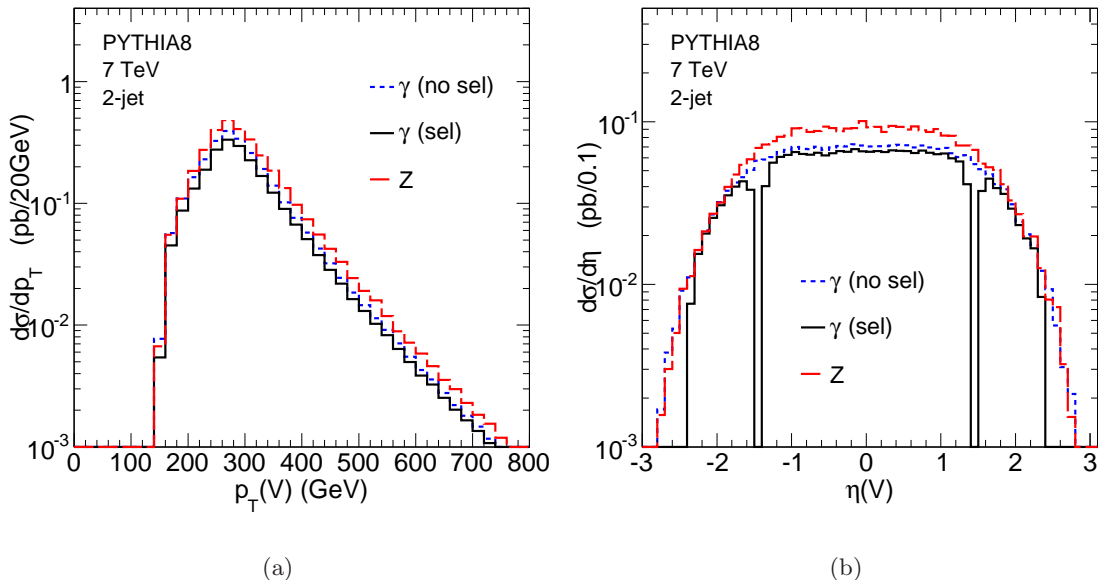


Figure 12. (a) Boson p_T and (b) η distributions from events passing the 2-jet SUSY selection. Results from photon events both with (sel) and without (no sel) applying the photon analysis selection are shown together with results from Z events (Z).

This section demonstrates the estimation of $Z \rightarrow \nu\bar{\nu}$ background for a zero lepton SUSY search using photon events. This is done using the PYTHIA8 results and is meant to serve as a general example, since the method could be used also for other new physics searches where $Z \rightarrow \nu\bar{\nu}$ production contributes with a significant background. The method involves the following steps:

- Photon event selection. Select a photon event sample using a loose enough selection, with respect to the photon and jets, to contain as many events as possible that will pass the final selection. This is represented here by the criteria $p_T(\gamma) > 45$ GeV, $|\eta(\gamma)| < 2.37$, excluding $1.37 < |\eta(\gamma)| < 1.52$ and $E_T^{iso} < 4$ GeV, based on the ATLAS photon analysis [17, 18].
- SUSY event selection. Apply the SUSY selection to the photon events, where the photon p_T represents the missing transverse energy from the Z in the events to be estimated. A 2-jet as well as 3-jet SUSY selection is used, based on the ATLAS search. 2-jet (3-jet): $p_T(j_1) > 120$ GeV, $p_T(j_2) > 40$ GeV, ($p_T(j_3) > 40$ GeV), $|\eta(j_i)| < 2.5$, $p_T(V) > 100$ GeV, $\Delta\phi(V, j_i) > 0.4$, $p_T(V)/m_{eff} > 0.3$ and $m_{eff} > 500$

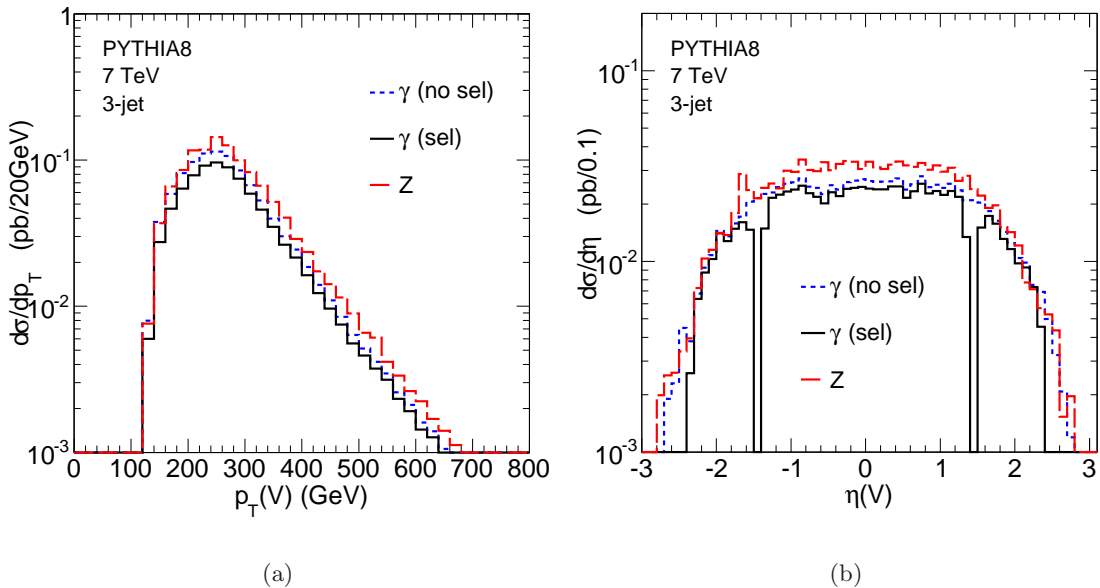


Figure 13. (a) Boson p_T and (b) η distributions from events passing the 3-jet SUSY selection. Results from photon events both with (sel) and without (no sel) applying the photon analysis selection are shown together with results from Z events (Z).

GeV. Here j_i represents the i^{th} leading jet and m_{eff} is the SUSY discriminating variable used in [1, 2], defined as the scalar sum of the p_T from the jets and the boson in the event.

- Subtract backgrounds and correct for experimental efficiencies. This is represented here only by the isolation efficiency.
- Convert photon events, inside the acceptance of the analysis, to $Z_{\nu\nu}$ events using the cross section ratio, $R(p_T^V) \cdot Br(Z \rightarrow \nu\nu)$. As discussed in the previous sections, in an analysis of real LHC data, $R(p_T^V)$ should be based on results from exact multijet MEs and using an appropriate jet selection.
- Correct for acceptance constraints implied by the photon analysis, e.g. the $\eta(\gamma)$ selection criteria.

The main intention with this method is that all necessary corrections as well as theoretical input are related to the vector bosons, whereas all requirements with respect to the experimentally more challenging reconstructed jets, are identical for the Z and γ events. As shown in the previous section, the ratio is affected by requiring jets. However, since this effect is a consequence of changing the mixture of couplings imposed by the relevant initial partons together with their PDFs, it is small even for drastically different jet criteria and should be yet smaller with respect to experimental jet uncertainties, such as energy scale and resolution.

The photon event selection imposes some unavoidable criteria which are not experienced by the $Z_{\nu\nu}$ background and therefore has to be corrected for. The implications of this selection on the final sample are, however, relatively mild for the following reasons. The photon p_T requirement is significantly softer than the subsequent selection. A photon isolation criterion, of some kind, is required in order to obtain accurate calculations of the ratio. However, this is often also used in the SUSY selection for more experimental reasons, such as to prevent fake missing transverse energy caused by a high p_T jet, i.e. the $\Delta\phi(V, j_i)$ requirement above. In addition, the fact that the Z and γ processes have the same phase space when $p_T \gg M_Z$ means that at high p_T , the η distributions from the γ and Z events converge toward the same distribution, which becomes increasingly central with higher boson p_T . Therefore any acceptance corrections will become the same for the Z as for the γ events.

The SUSY selection, based on the p_T of the boson and jets in the event, is then identical for the two event types and should not require any related corrections. Due to the fact that the bosons are recoiling against the hadrons, the SUSY selection will in principle act as a non-trivial high boson p_T criteria. For this reason the γ events passing the SUSY selection can be converted into Z events based only on the boson kinematics. Again due to the convergence of the Z and γ phase space at high p_T , the cross section ratio becomes insensitive to the particular $\eta(V)$ criteria used and is hence determined by the $p_T(V)$. The precision of this method is therefore mainly related to the photon analysis part, which is expected to be precise at high photon p_T , and the theoretical knowledge of the Z/γ cross section ratio.

In figures 12 and 13 the boson p_T and η distributions are shown after the 2-jet and 3-jet SUSY selections respectively. The distributions for photon events, with (sel) and without (no sel) passing the photon selection, as well as Z events (Z) are shown. The p_T distributions show that both the SUSY selections mainly select events with a boson p_T in the range 250 to 300 GeV. The η distributions also show the similarity in shape of the distributions from the Z and γ processes. Both the p_T and η distributions show that the effect from the photon selection, i.e. acceptance and isolation requirements, is relatively small also after the SUSY selection and the difference between the Z and γ results is consistent with the cross section ratio at relevant boson p_T values. In the η distributions, the difference from applying the photon selection reflects the impact of the isolation criteria alone and it is shown that the additional jet requirements from the SUSY selections do not change the isolation efficiency dramatically. The results from the 2-jet and 3-jet selections do have slight differences, but the overall characteristics discussed are the same. Figure 14 shows the Z p_T distributions from γ events passing the two SUSY selections, converted into $Z \rightarrow \nu\bar{\nu}$ according to the method outlined above, together with the results obtained from simulating $Z \rightarrow \nu\bar{\nu}$ directly. Since the PYTHIA8 ratios do not show any jet multiplicity dependence, the ratio shown in figure 11 (reco) was used in this analysis example for both the 2-jet and 3-jet results. As expected, the two distributions agree within the statistical uncertainty of the simulation, which is smaller than 5% in the bulk of the distributions.

The uncertainties on the final background estimate, related to the experimental aspects of this analysis, are not covered by this study. However, as discussed above, the design

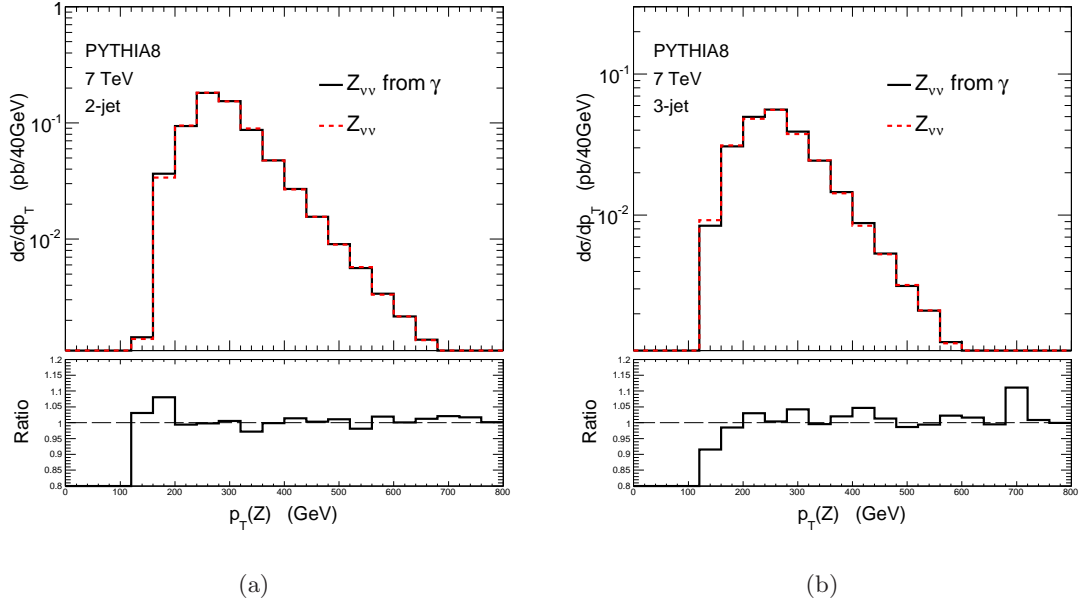


Figure 14. Differential cross section as a function of $p_T(Z)$ for $Z \rightarrow \nu\nu$ events passing the (a) 2-jet and (b) 3-jet SUSY selection. The predictions using γ events ($Z_{\nu\nu}$ from γ) are compared to results from direct MC simulation of the $Z \rightarrow \nu\bar{\nu}$ process ($Z_{\nu\nu}$).

of the method should limit the exposure mainly to the corrections from the photon event selection, which are expected to be precise at high boson p_T . In addition, as discussed in section 4.1, the impact associated with full event simulation on the cross section ratio was found to be small. As shown in figure 11(b), the ratio increases, by about 6% in the high p_T region, when including the isolation efficiency, whereas a significantly smaller effect is seen when going from parton to particle level. The final uncertainties on $R(Z/\gamma)$ from such effects are therefore expected to be at the percent level. A theoretical uncertainty, here with respect to the hard process calculations behind $R(Z/\gamma) \cdot Br(Z \rightarrow \nu\nu)$, that significantly exceeds 10% is therefore likely to dominate the uncertainty of the method.

Table 1 presents the overall $R \cdot Br$ values obtained for the results shown in figure 14. This includes both the value from PYTHIA8 (R^P), that was actually used in the plot, as well as the corrected value (R^{ME}) based on the ME results. The table also includes the uncertainties associated with the ME calculation (ε_{ME}), the scales (ε_μ) and the PDFs (ε_{PDF}), see section 3. The results show a total uncertainty of $\pm 7\%$ and indicate that the theoretical uncertainty for results obtained by an appropriately configured MC program, which uses ME amplitudes for the hard jets, should be within 10%. The SUSY selection used in the experimental analysis will evolve with an increasing amount of LHC data. However, such an evolution is expected to effectively imply a harder boson p_T requirement and since the uncertainties in table 1 are valid for $p_T(V) > 100$ GeV, the same conclusions should hold also for harder selections.⁶

⁶At least up to $p_T(V) = 800$ GeV, which is the maximum value included in this study.

Selection	$R^P \cdot Br$	$R^{ME} \cdot Br$	ε_{ME}	ε_μ	ε_{PDF}	ε_{Tot}
2-jet	0.254	0.234	5%	3%	4%	7%
3-jet	0.246	0.207	5%	3%	4%	7%

Table 1. The overall $R \cdot Br$ values obtained after the SUSY selections, directly from PYTHIA8 (R^P) as well as corrected values with respect to the ME results (R^{ME}). The uncertainties associated with the ME calculation (ε_{ME}), the scales (ε_μ) and the PDFs (ε_{PDF}) are also shown.

5 Summary and conclusions

One of the best methods to calibrate the irreducible background from $Z(\rightarrow \nu\nu)+\text{jets}$, to beyond the SM searches at the LHC, comes from using $\gamma+\text{jets}$ data. The method utilises the fact that at high boson p_T ($\gg M_Z$) the event kinematics converge for the two processes and the cross sections differ mainly due to the boson couplings. The advantage comes from large statistics, compared to alternative methods using $Z(\rightarrow ee, \mu\mu)+\text{jets}$ events, together with the clean signature, with respect to experimental efficiencies and background, at high photon p_T . Hence, a precise prediction from theory of the Z/γ cross section ratio, $R(Z/\gamma)$, is required. The similarity between the two processes should allow for a robust prediction of $R(Z/\gamma)$, given careful attention to the modelling of the jets.

The general dependence of $R(Z/\gamma)$ on the mixture of boson couplings, which is determined by the initial state partons of the relevant amplitudes and their corresponding PDFs, has been illustrated. Relatively accurate values can be obtained even using rough approximations in the 1-jet case, whereas a larger set of amplitudes becomes necessary when 2 or more jets are required. The ratios have been studied at parton level using both the (LO) PYTHIA8 as well as the (multijet ME) GAMBOS programs, which allows us to disentangle effects associated with the two approaches. The impact from exact MEs when requiring different numbers of jets was found to be significant, but uncertainties were found to be within 5% for the acceptance from typical experimental cuts. The corresponding uncertainties related to the PDFs and scale choice were found to be less than 4% and 3% respectively.

The PYTHIA8 MC program was used to investigate effects on $R(Z/\gamma)$ associated with full event simulation as well as performing a proof of principle analysis example. The effects investigated were found to be small and indicate that a theoretical precision⁷ at the 10% level is required, in order not to significantly degrade the performance of the method. The total theoretical uncertainty was found to be 7%, indicating that the results obtained by MC simulations, including exact multijet MEs, should be within the 10% level. These results should also hold for similar 2- and 3-jet selections, given that the effective p_T requirement on the boson is harder than what is used in the example analysis. Note that all our theoretical cross sections are evaluated in leading-order pQCD. It will be important to check, using for example the techniques of [10], that the ratio predictions are indeed stable – at least to the required accuracy – with respect to higher-order pQCD corrections.

⁷Again, referring to the hard QCD process calculations behind $R \cdot Br$.

Finally, one type of correction that has not been included in our theoretical study is high-order electroweak corrections. Although these are intrinsically small, and many will again cancel in the Z/γ ratio, there is an important class of correction involving W and Z virtual exchanges that does not cancel in the ratio. The impact on both the Z and γ distributions have been studied in [23, 24]. It was shown that non-cancelling Sudakov-type logarithms $\sim \alpha \log^2(p_T(V)^2/m_W^2)$ appear at high $p_T(V)$, and decrease the $Z/\gamma + 1$ jet ratio by 6% (11%) at $p_T(V) = 300$ (800) GeV [24]. However care is needed in the interpretation of this result, since the emission of *real* W bosons is expected to compensate the virtual Sudakov logarithms to some extent [25, 26]. It is therefore important to carry out a full analysis of higher-order electroweak corrections for the multijet processes and acceptance cuts studied in this paper.

Acknowledgments

This work was supported in part by the EU Marie Curie Research Training Network “MC-net”, under contract number MRTN-CT-2006-035606, the UK Science and Technology Facilities Council and by the Mexican Council of Science and Technology (CONACYT). Useful correspondence with Markus Schulze is acknowledged.

References

- [1] ATLAS Collaboration, *Search for squarks and gluinos using final states with jets and missing transverse momentum with the ATLAS detector in $\sqrt{s} = 7$ TeV proton-proton collisions*, arXiv:1102.5290v1 [hep-ex], Submitted to Phys. Lett. B.
- [2] ATLAS Collaboration, *Search for squarks and gluinos using final states with jets and missing transverse momentum with the ATLAS detector in $\sqrt{s} = 7$ TeV proton-proton collisions*, ATLAS-CONF-2011-086.
- [3] CMS Collaboration, *Data-Driven Estimation of the Invisible Z Background to the SUSY MET Plus Jets Search*, CMS-PAS-SUS-08-002.
- [4] CMS Collaboration, *Search for Supersymmetry in pp Collisions at 7 TeV in Events with Jets and Missing Transverse Energy*, Phys. Lett. **B698** (2011) 196 [arXiv:1101.1628v2 [hep-ex]].
- [5] CMS Collaboration, *Search for New Physics with Jets and Missing Transverse Momentum in pp collisions at $\sqrt{s} = 7$ TeV*, arXiv:1106.4503v1 [hep-ex], Submitted to JHEP.
- [6] CDF Collaboration, *First Observation of Vector Boson Pairs in a Hadronic Final State at the Tevatron Collider*, Phys. Rev. Lett. **103** (2009) 091803 [arXiv:0905.4714v1 [hep-ex]].
- [7] T. Sjöstrand, S. Mrenna and P. Skands, *PYTHIA 6.4 Physics and Manual*, JHEP **0605** (2006) 026 [arXiv:hep-ph/0603175v2].
- [8] T. Sjöstrand, S. Mrenna and P. Skands, *A Brief Introduction to PYTHIA 8.1*, Comput. Phys. Comm. **178** (2008) 852 [arXiv:0710.3820v1 [hep-ph]].
- [9] M. Bähr et al., *Herwig++ Physics and Manual*, Eur. Phys. J. **C58** (2008) 639 [arXiv:0803.0883v3 [hep-ph]].
- [10] Z. Bern et al., *Driving Missing Data at Next-to-Leading Order*, arXiv:1106.1423v1 [hep-ph].

- [11] T. Gleisberg et al., *Event generation with SHERPA 1.1*, JHEP **0902** (2009) 007 [arXiv:0811.4622v1 [hep-ph]].
- [12] R. K. Ellis, W. J. Stirling and B. R. Webber, *QCD and Collider Physics*, Cambridge University Press, Cambridge U.K. (1996).
- [13] A. D. Martin, W. J. Stirling, R. S. Thorne and G. Watt, *Parton distributions for the LHC*, Eur. Phys. J. **C63** (2009) 189 [arXiv:0901.0002 [hep-ph]].
- [14] F. A. Berends, H. Kuijf, B. Tausk and W. T. Giele, *On the production of a W and jets at hadron colliders*, Nucl. Phys. **B357** (1991) 32.
- [15] H. L. Lai et al., *Global QCD analysis of parton structure of the nucleon: CTEQ5 parton distributions*, Eur. Phys. J. **C12** (2000) 375 [arXiv:hep-ph/9903282v3].
- [16] M. Glück, E. Reya and A. Vogt, *Dynamical parton distributions revisited*, Eur. Phys. J. **C5** (1998) 461 [arXiv:hep-ph/9806404v1].
- [17] ATLAS Collaboration, *Measurement of the inclusive isolated prompt photon cross section in pp collisions at $\sqrt{s} = 7$ TeV with the ATLAS detector*, Phys. Rev. **D83** (2011) 052005 [arXiv:1012.4389v2 [hep-ex]].
- [18] ATLAS Collaboration, *Measurement of the inclusive isolated prompt photon cross section in pp collisions at $\sqrt{s} = 7$ TeV with the ATLAS detector using 35 pb⁻¹*, ATLAS-CONF-2011-058.
- [19] A. Buckley, et al., *General-purpose event generators for LHC physics*, Phys. Rept. **504** (2011) 145 [arXiv:1101.2599v1 [hep-ph]].
- [20] M. Cacciari, G. P. Salam and G. Soyez, *The Anti-k(t) jet clustering algorithm*, JHEP **0804** (2008) 063 [arXiv:0802.1189v2 [hep-ph]].
- [21] M. Cacciari, G. P. Salam, *Dispelling the N³ myth for the k_t jet-finder*, Phys. Lett. **B641** (2006) 57 [arXiv:hep-ph/0512210v2].
- [22] M. Cacciari, G. P. Salam and G. Soyez, <http://fastjet.fr>.
- [23] E. Maina, S. Moretti and D. A. Ross, *One loop weak corrections to gamma / Z hadroproduction at finite transverse momentum*, Phys. Lett. B **593** (2004) 143 [Erratum-ibid. B **614** (2005) 216] [arXiv:hep-ph/0403050].
- [24] J. H. Kuhn, A. Kulesza, S. Pozzorini and M. Schulze, *Electroweak corrections to hadronic photon production at large transverse momenta*, JHEP **0603** (2006) 059 [arXiv:hep-ph/0508253].
- [25] U. Baur, *Weak Boson Emission in Hadron Collider Processes*, Phys. Rev. **D75** (2007) 013005. [hep-ph/0611241].
- [26] G. Bell, J. H. Kuhn, J. Rittinger, *Electroweak Sudakov Logarithms and Real Gauge-Boson Radiation in the TeV Region*, Eur. Phys. J. **C70** (2010) 659-671. [arXiv:1004.4117 [hep-ph]].